

A Search for $B^- \rightarrow \tau^- \bar{\nu}$ Recoiling Against a Fully Reconstructed B

The BABAR Collaboration

November 20, 2018

Abstract

We present a search for the $B^- \rightarrow \tau^- \bar{\nu}$ decay in a data sample of 82 fb^{-1} collected at the $\Upsilon(4S)$ resonance with the BABAR detector at the SLAC PEP-II asymmetric B Factory. Continuum and combinatorial backgrounds are suppressed by selecting a sample of events with one completely reconstructed B . The decay products of the other B in the event are analyzed to search for a $B^- \rightarrow \tau^- \bar{\nu}$ decay. The τ lepton is identified in the following decay channels: $\tau^- \rightarrow e^- \nu \bar{\nu}$, $\tau^- \rightarrow \mu^- \nu \bar{\nu}$, $\tau^- \rightarrow \pi^- \nu$, $\tau^- \rightarrow \pi^- \pi^0 \nu$, $\tau^- \rightarrow \pi^- \pi^+ \pi^- \nu$. We find no evidence for a signal and set a 90% C.L. upper limit of $\mathcal{B}(B^- \rightarrow \tau^- \bar{\nu}) < 7.7 \times 10^{-4}$. We combine this result with another BABAR measurement searching for $B^- \rightarrow \tau^- \bar{\nu}$ decays in a sample with one B meson reconstructed in semi-leptonic channels. The two samples are statistically independent. We obtain a combined 90% C.L. upper limit of $\mathcal{B}(B^- \rightarrow \tau^- \bar{\nu}) < 4.1 \times 10^{-4}$. All results are preliminary.

Presented at the XXXVIIIth Rencontres de Moriond on
Electroweak Interactions and Unified Theories,
3/15—3/22/2003, Les Arcs, Savoie, France

Stanford Linear Accelerator Center, Stanford University, Stanford, CA 94309

Work supported in part by Department of Energy contract DE-AC03-76SF00515.

The BABAR Collaboration,

B. Aubert, R. Barate, D. Boutigny, J.-M. Gaillard, A. Hicheur, Y. Karyotakis, J. P. Lees, P. Robbe,
V. Tisserand, A. Zghiche

Laboratoire de Physique des Particules, F-74941 Annecy-le-Vieux, France

A. Palano, A. Pompili

Università di Bari, Dipartimento di Fisica and INFN, I-70126 Bari, Italy

J. C. Chen, N. D. Qi, G. Rong, P. Wang, Y. S. Zhu

Institute of High Energy Physics, Beijing 100039, China

G. Eigen, I. Ofte, B. Stugu

University of Bergen, Inst. of Physics, N-5007 Bergen, Norway

G. S. Abrams, A. W. Borgland, A. B. Breon, D. N. Brown, J. Button-Shafer, R. N. Cahn, E. Charles,
C. T. Day, M. S. Gill, A. V. Gritsan, Y. Groysman, R. G. Jacobsen, R. W. Kadel, J. Kadyk, L. T. Kerth,
Yu. G. Kolomensky, J. F. Kral, G. Kukartsev, C. LeClerc, M. E. Levi, G. Lynch, L. M. Mir, P. J. Oddone,
T. J. Orimoto, M. Pripstein, N. A. Roe, A. Romosan, M. T. Ronan, V. G. Shelkov, A. V. Telnov,
W. A. Wenzel

Lawrence Berkeley National Laboratory and University of California, Berkeley, CA 94720, USA

T. J. Harrison, C. M. Hawkes, D. J. Knowles, R. C. Penny, A. T. Watson, N. K. Watson

University of Birmingham, Birmingham, B15 2TT, United Kingdom

T. Deppermann, K. Goetzen, H. Koch, B. Lewandowski, M. Pelizaeus, K. Peters, H. Schmuecker,
M. Steinke

Ruhr Universität Bochum, Institut für Experimentalphysik 1, D-44780 Bochum, Germany

N. R. Barlow, W. Bhimji, J. T. Boyd, N. Chevalier, W. N. Cottingham, C. Mackay, F. F. Wilson

University of Bristol, Bristol BS8 1TL, United Kingdom

C. Hearty, T. S. Mattison, J. A. McKenna, D. Thiessen

University of British Columbia, Vancouver, BC, Canada V6T 1Z1

P. Kyberd, A. K. McKemey

Brunel University, Uxbridge, Middlesex UB8 3PH, United Kingdom

V. E. Blinov, A. D. Bukin, V. B. Golubev, V. N. Ivanchenko, E. A. Kravchenko, A. P. Onuchin,
S. I. Serednyakov, Yu. I. Skovpen, E. P. Solodov, A. N. Yushkov

Budker Institute of Nuclear Physics, Novosibirsk 630090, Russia

D. Best, M. Chao, D. Kirkby, A. J. Lankford, M. Mandelkern, S. McMahon, R. K. Mommsen, W. Roethel,
D. P. Stoker

University of California at Irvine, Irvine, CA 92697, USA

C. Buchanan

University of California at Los Angeles, Los Angeles, CA 90024, USA

H. K. Hadavand, E. J. Hill, D. B. MacFarlane, H. P. Paar, Sh. Rahatlou, U. Schwanke, V. Sharma

University of California at San Diego, La Jolla, CA 92093, USA

J. W. Berryhill, C. Campagnari, B. Dahmes, N. Kuznetsova, S. L. Levy, O. Long, A. Lu, M. A. Mazur,
J. D. Richman, W. Verkerke

University of California at Santa Barbara, Santa Barbara, CA 93106, USA

J. Beringer, A. M. Eisner, C. A. Heusch, W. S. Lockman, T. Schalk, R. E. Schmitz, B. A. Schumm,
A. Seiden, M. Turri, W. Walkowiak, D. C. Williams, M. G. Wilson

University of California at Santa Cruz, Institute for Particle Physics, Santa Cruz, CA 95064, USA

J. Albert, E. Chen, M. P. Dorsten, G. P. Dubois-Felsmann, A. Dvoretzskii, D. G. Hitlin, I. Narsky,
F. C. Porter, A. Ryd, A. Samuel, S. Yang

California Institute of Technology, Pasadena, CA 91125, USA

S. Jayatilleke, G. Mancinelli, B. T. Meadows, M. D. Sokoloff

University of Cincinnati, Cincinnati, OH 45221, USA

T. Barillari, F. Blanc, P. Bloom, P. J. Clark, W. T. Ford, U. Nauenberg, A. Olivas, P. Rankin, J. Roy,
J. G. Smith, W. C. van Hoek, L. Zhang

University of Colorado, Boulder, CO 80309, USA

J. L. Harton, T. Hu, A. Soffer, W. H. Toki, R. J. Wilson, J. Zhang

Colorado State University, Fort Collins, CO 80523, USA

D. Altenburg, T. Brandt, J. Brose, T. Colberg, M. Dickopp, R. S. Dubitzky, A. Hauke, H. M. Lacker,
E. Maly, R. Müller-Pfefferkorn, R. Nogowski, S. Otto, K. R. Schubert, R. Schwierz, B. Spaan, L. Wilden

Technische Universität Dresden, Institut für Kern- und Teilchenphysik, D-01062 Dresden, Germany

D. Bernard, G. R. Bonneaud, F. Brochard, J. Cohen-Tanugi, Ch. Thiebaux, G. Vasileiadis, M. Verderi

Ecole Polytechnique, LLR, F-91128 Palaiseau, France

A. Khan, D. Lavin, F. Muheim, S. Playfer, J. E. Swain, J. Tinslay

University of Edinburgh, Edinburgh EH9 3JZ, United Kingdom

C. Bozzi, L. Piemontese, A. Sarti

Università di Ferrara, Dipartimento di Fisica and INFN, I-44100 Ferrara, Italy

E. Treadwell

Florida A&M University, Tallahassee, FL 32307, USA

F. Anulli,¹ R. Baldini-Ferroli, A. Calcaterra, R. de Sangro, D. Falciari, G. Finocchiaro, P. Patteri,
I. M. Peruzzi,¹ M. Piccolo, A. Zallo

Laboratori Nazionali di Frascati dell'INFN, I-00044 Frascati, Italy

A. Buzzo, R. Contri, G. Crosetti, M. Lo Vetere, M. Macri, M. R. Monge, S. Passaggio, F. C. Pastore,
C. Patrignani, E. Robutti, A. Santroni, S. Tosi

Università di Genova, Dipartimento di Fisica and INFN, I-16146 Genova, Italy

S. Bailey, M. Morii

Harvard University, Cambridge, MA 02138, USA

¹Also with Università di Perugia, Perugia, Italy

G. J. Grenier, S.-J. Lee, U. Mallik
University of Iowa, Iowa City, IA 52242, USA

J. Cochran, H. B. Crawley, J. Lamsa, W. T. Meyer, S. Prell, E. I. Rosenberg, J. Yi
Iowa State University, Ames, IA 50011-3160, USA

M. Davier, G. Grosdidier, A. Höcker, S. Laplace, F. Le Diberder, V. Lepeltier, A. M. Lutz, T. C. Petersen,
S. Plaszczynski, M. H. Schune, L. Tantot, G. Wormser
Laboratoire de l'Accélérateur Linéaire, F-91898 Orsay, France

R. M. Bionta, V. Brigljević, C. H. Cheng, D. J. Lange, D. M. Wright
Lawrence Livermore National Laboratory, Livermore, CA 94550, USA

A. J. Bevan, J. R. Fry, E. Gabathuler, R. Gamet, M. Kay, D. J. Payne, R. J. Sloane, C. Touramanis
University of Liverpool, Liverpool L69 3BX, United Kingdom

M. L. Aspinwall, D. A. Bowerman, P. D. Dauncey, U. Egede, I. Eschrich, G. W. Morton, J. A. Nash,
P. Sanders, G. P. Taylor
University of London, Imperial College, London, SW7 2BW, United Kingdom

J. J. Back, G. Bellodi, P. F. Harrison, H. W. Shorthouse, P. Strother, P. B. Vidal
Queen Mary, University of London, E1 4NS, United Kingdom

G. Cowan, H. U. Flaecher, S. George, M. G. Green, A. Kurup, C. E. Marker, T. R. McMahon, S. Ricciardi,
F. Salvatore, G. Vaitsas, M. A. Winter
*University of London, Royal Holloway and Bedford New College, Egham, Surrey TW20 0EX,
United Kingdom*

D. Brown, C. L. Davis
University of Louisville, Louisville, KY 40292, USA

J. Allison, R. J. Barlow, A. C. Forti, P. A. Hart, F. Jackson, G. D. Lafferty, A. J. Lyon, J. H. Weatherall,
J. C. Williams
University of Manchester, Manchester M13 9PL, United Kingdom

A. Farbin, A. Jawahery, D. Kovalskyi, C. K. Lae, V. Lillard, D. A. Roberts
University of Maryland, College Park, MD 20742, USA

G. Blaylock, C. Dallapiccola, K. T. Flood, S. S. Hertzbach, R. Kofler, V. B. Koptchev, T. B. Moore,
H. Staengle, S. Willocq
University of Massachusetts, Amherst, MA 01003, USA

R. Cowan, G. Sciolla, F. Taylor, R. K. Yamamoto
Massachusetts Institute of Technology, Laboratory for Nuclear Science, Cambridge, MA 02139, USA

D. J. J. Mangeol, M. Milek, P. M. Patel
McGill University, Montréal, QC, Canada H3A 2T8

A. Lazzaro, F. Palombo
Università di Milano, Dipartimento di Fisica and INFN, I-20133 Milano, Italy

J. M. Bauer, L. Cremaldi, V. Eschenburg, R. Godang, R. Kroeger, J. Reidy, D. A. Sanders, D. J. Summers,
H. W. Zhao

University of Mississippi, University, MS 38677, USA

C. Hast, P. Taras

Université de Montréal, Laboratoire René J. A. Lévesque, Montréal, QC, Canada H3C 3J7

H. Nicholson

Mount Holyoke College, South Hadley, MA 01075, USA

C. Cartaro, N. Cavallo, G. De Nardo, F. Fabozzi,² C. Gatto, L. Lista, P. Paolucci, D. Piccolo, C. Sciacca
Università di Napoli Federico II, Dipartimento di Scienze Fisiche and INFN, I-80126, Napoli, Italy

M. A. Baak, G. Raven

*NIKHEF, National Institute for Nuclear Physics and High Energy Physics, 1009 DB Amsterdam,
The Netherlands*

J. M. LoSecco

University of Notre Dame, Notre Dame, IN 46556, USA

T. A. Gabriel

Oak Ridge National Laboratory, Oak Ridge, TN 37831, USA

B. Brau, T. Pulliam

Ohio State University, Columbus, OH 43210, USA

J. Brau, R. Frey, M. Iwasaki, C. T. Potter, N. B. Sinev, D. Strom, E. Torrence

University of Oregon, Eugene, OR 97403, USA

F. Colecchia, A. Dorigo, F. Galeazzi, M. Margoni, M. Morandin, M. Posocco, M. Rotondo, F. Simonetto,
R. Stroili, G. Tiozzo, C. Voci

Università di Padova, Dipartimento di Fisica and INFN, I-35131 Padova, Italy

M. Benayoun, H. Briand, J. Chauveau, P. David, Ch. de la Vaissière, L. Del Buono, O. Hamon,
Ph. Leruste, J. Ocariz, M. Pivk, L. Roos, J. Stark, S. T'Jampens

Universités Paris VI et VII, Lab de Physique Nucléaire H. E., F-75252 Paris, France

P. F. Manfredi, V. Re

Università di Pavia, Dipartimento di Elettronica and INFN, I-27100 Pavia, Italy

L. Gladney, Q. H. Guo, J. Panetta

University of Pennsylvania, Philadelphia, PA 19104, USA

C. Angelini, G. Batignani, S. Bettarini, M. Bondioli, F. Bucci, G. Calderini, M. Carpinelli, F. Forti,
M. A. Giorgi, A. Lusiani, G. Marchiori, F. Martinez-Vidal,³ M. Morganti, N. Neri, E. Paoloni, M. Rama,
G. Rizzo, F. Sandrelli, J. Walsh

Università di Pisa, Dipartimento di Fisica, Scuola Normale Superiore and INFN, I-56127 Pisa, Italy

²Also with Università della Basilicata, Potenza, Italy

³Also with IFIC, Instituto de Física Corpuscular, CSIC-Universidad de Valencia, Valencia, Spain

M. Haire, D. Judd, K. Paick, D. E. Wagoner
Prairie View A&M University, Prairie View, TX 77446, USA

N. Danielson, P. Elmer, C. Lu, V. Miftakov, J. Olsen, A. J. S. Smith, E. W. Varnes
Princeton University, Princeton, NJ 08544, USA

F. Bellini, G. Cavoto,⁴ D. del Re, R. Faccini,⁵ F. Ferrarotto, F. Ferroni, M. Gaspero, E. Leonardi,
M. A. Mazzoni, S. Morganti, M. Pierini, G. Piredda, F. Safai Tehrani, M. Serra, C. Voena
Università di Roma La Sapienza, Dipartimento di Fisica and INFN, I-00185 Roma, Italy

S. Christ, G. Wagner, R. Waldi
Universität Rostock, D-18051 Rostock, Germany

T. Adye, N. De Groot, B. Franek, N. I. Geddes, G. P. Gopal, E. O. Olaiya, S. M. Xella
Rutherford Appleton Laboratory, Chilton, Didcot, Oxon, OX11 0QX, United Kingdom

R. Aleksan, S. Emery, A. Gaidot, S. F. Ganzhur, P.-F. Giraud, G. Hamel de Monchenault, W. Kozanecki,
M. Langer, G. W. London, B. Mayer, G. Schott, G. Vasseur, Ch. Yeche, M. Zito
DAPNIA, Commissariat à l'Energie Atomique/Saclay, F-91191 Gif-sur-Yvette, France

M. V. Purohit, A. W. Weidemann, F. X. Yumiceva
University of South Carolina, Columbia, SC 29208, USA

D. Aston, R. Bartoldus, N. Berger, A. M. Boyarski, O. L. Buchmueller, M. R. Convery, D. P. Coupal,
D. Dong, J. Dorfan, D. Dujmic, W. Dunwoodie, R. C. Field, T. Glanzman, S. J. Gowdy, E. Grauges-Pous,
T. Hadig, V. Halyo, T. Hryn'ova, W. R. Innes, C. P. Jessop, M. H. Kelsey, P. Kim, M. L. Kocian,
U. Langenegger, D. W. G. S. Leith, S. Luitz, V. Luth, H. L. Lynch, H. Marsiske, S. Menke, R. Messner,
D. R. Muller, C. P. O'Grady, V. E. Ozcan, A. Perazzo, M. Perl, S. Petrak, B. N. Ratcliff, S. H. Robertson,
A. Roodman, A. A. Salnikov, R. H. Schindler, J. Schwiening, G. Simi, A. Snyder, A. Soha, J. Stelzer,
D. Su, M. K. Sullivan, H. A. Tanaka, J. Va'vra, S. R. Wagner, M. Weaver, A. J. R. Weinstein,
W. J. Wisniewski, D. H. Wright, C. C. Young
Stanford Linear Accelerator Center, Stanford, CA 94309, USA

P. R. Burchat, T. I. Meyer, C. Roat
Stanford University, Stanford, CA 94305-4060, USA

S. Ahmed, J. A. Ernst
State Univ. of New York, Albany, NY 12222, USA

W. Bugg, M. Krishnamurthy, S. M. Spanier
University of Tennessee, Knoxville, TN 37996, USA

R. Eckmann, H. Kim, J. L. Ritchie, R. F. Schwitters
University of Texas at Austin, Austin, TX 78712, USA

J. M. Izen, I. Kitayama, X. C. Lou, S. Ye
University of Texas at Dallas, Richardson, TX 75083, USA

⁴Also with Princeton University, Princeton, NJ 08544, USA

⁵Also with University of California at San Diego, La Jolla, CA 92093, USA

F. Bianchi, M. Bona, F. Gallo, D. Gamba

Università di Torino, Dipartimento di Fisica Sperimentale and INFN, I-10125 Torino, Italy

C. Borean, L. Bosisio, G. Della Ricca, S. Dittongo, S. Grancagnolo, L. Lanceri, P. Poropat,⁶ L. Vitale,
G. Vuagnin

Università di Trieste, Dipartimento di Fisica and INFN, I-34127 Trieste, Italy

R. S. Panvini

Vanderbilt University, Nashville, TN 37235, USA

Sw. Banerjee, C. M. Brown, D. Fortin, P. D. Jackson, R. Kowalewski, J. M. Roney

University of Victoria, Victoria, BC, Canada V8W 3P6

H. R. Band, S. Dasu, M. Datta, A. M. Eichenbaum, H. Hu, J. R. Johnson, R. Liu, F. Di Lodovico,
A. K. Mohapatra, Y. Pan, R. Prepost, S. J. Sekula, J. H. von Wimmersperg-Toeller, J. Wu, S. L. Wu, Z. Yu

University of Wisconsin, Madison, WI 53706, USA

H. Neal

Yale University, New Haven, CT 06511, USA

⁶Deceased

1 Introduction

The study of the leptonic decay $B^- \rightarrow \ell^- \bar{\nu}$ ¹ is of particular interest because it is sensitive to the product of the Cabibbo-Kobayashi-Maskawa matrix element $|V_{ub}|$ and the B meson decay constant f_B , which describes the overlap of the quark wave functions inside the B meson and is only known from theory [1]. The knowledge of f_B is essential for the extraction of the Cabibbo-Kobayashi-Maskawa matrix element $|V_{td}|$ from processes of $B^0 \bar{B}^0$ mixing in which the oscillation frequency is proportional to f_B^2 . In the Standard Model the amplitude of the $B^- \rightarrow \ell^- \bar{\nu}$ decay is due to the annihilation of the b and \bar{u} quarks into a virtual W boson. The resulting expression for the branching fraction is:

$$\mathcal{B}(B^- \rightarrow \ell^- \bar{\nu}) = \frac{G_F^2 m_B}{8\pi} m_\ell^2 \left(1 - \frac{m_\ell^2}{m_B^2}\right)^2 f_B^2 |V_{ub}|^2 \tau_B, \quad (1)$$

where G_F is the Fermi coupling constant, m_ℓ and m_B are the charged lepton and B meson masses, τ_B is the B^- lifetime. The dependence of $\mathcal{B}(B^- \rightarrow \ell^- \bar{\nu})$ on the lepton mass arises from helicity conservation, which strongly suppresses the muon and electron channels. Using data from Ref. [2], the Standard Model expectation in Eq. (1) for the τ channel becomes:

$$\mathcal{B}(B^- \rightarrow \tau^- \bar{\nu}) = (7.5 \times 10^{-5}) \frac{\tau_B}{1.674 \text{ ps}} \left(\frac{f_B}{198 \text{ MeV}}\right)^2 \left|\frac{V_{ub}}{0.0036}\right|^2. \quad (2)$$

While the theoretical dependence of the branching fraction from the relevant parameters, τ_B , f_B and V_{ub} , is straightforward, a search for the $B^- \rightarrow \tau^- \bar{\nu}$ decay is experimentally challenging due to the presence of additional undetectable neutrinos in the final state coming from the decay of the τ .

No observation of a $B^- \rightarrow \tau^- \bar{\nu}$ signal has been reported yet in the literature. The most stringent upper limit has been achieved by the L3 Collaboration [3]: $\mathcal{B}(B^- \rightarrow \tau^- \bar{\nu}) < 5.7 \times 10^{-4}$ at 90% C.L.

2 The *BABAR* detector and dataset

The data sample used in this analysis was recorded at the $\Upsilon(4S)$ resonance in 1999-2002 with the *BABAR* detector at the PEP-II asymmetric-energy e^+e^- collider at the Stanford Linear Accelerator Center. The integrated luminosity at the center of mass energies near $\Upsilon(4S)$ is 81.9 fb^{-1} , corresponding to 88.9 million $B\bar{B}$ pairs. We also used a Monte Carlo simulation of B^+B^- generic events with an equivalent luminosity of 136.9 fb^{-1} and of $\tau^+\tau^-$ events with an equivalent luminosity of 127.1 fb^{-1} .

The *BABAR* detector is described elsewhere [4]. Detection of charged particles and measurement of their momenta are performed using a combination of a five-layer silicon vertex tracker (SVT) and a 40-layer drift chamber (DCH) in a 1.5 T solenoidal magnetic field. A detector of internally-reflected Cherenkov radiation (DIRC) with a quartz bar radiator provides charged particle identification. A finely-segmented CsI(Tl) electromagnetic calorimeter (EMC) is used to detect photons and to identify electrons. The magnetic flux return system (IFR), which is instrumented with multiple layers of resistive plate chambers, provides muon and long-lived neutral hadron identification.

¹charge-conjugate modes are implied throughout the paper.

Charged kaons are identified from the observed pattern of Cherenkov light in the DIRC and from the dE/dx measurements in the SVT and DCH. Electron candidates are selected according to the ratio of EMC energy to track momentum, the EMC cluster shape, the dE/dx in the DCH and the DIRC Cherenkov angle, if available. Muon candidates are selected according to the difference between the expected and measured thickness of absorber traversed, the match of the hits in the IFR with the extrapolated track, the average and spread in the number of hits per IFR layer, and the energy deposited in the EMC.

3 Analysis method

We select a sample of events with one B meson (B_{reco}) completely reconstructed in a variety of hadronic decay modes. All the tracks and photon candidates in the event not used to reconstruct the B_{reco} are associated to the other B meson (recoil B) and are studied to search for a $B^- \rightarrow \tau^- \bar{\nu}$ signal.

The advantage of having a sample of fully reconstructed B_{reco} mesons is to provide a clean environment of B^+B^- events with a strong suppression of the combinatorial and continuum backgrounds. The drawback is a reduction of the data sample due to the low reconstruction efficiency.

3.1 Fully reconstructed B sample

The B_{reco} is reconstructed in a set of hadronic modes that can be summarized as $B^+ \rightarrow D^{(*)0} X^+$, where $D^{(*)0}$ is a charmed meson and X^+ is a system of charged and neutral hadrons composed by $n_1\pi^\pm + n_2K^\pm + n_3\pi^0 + n_4K_S^0$ ($n_1 = 1, \dots, 5$, $n_2 = 0, \dots, 2$, $n_3 = 0, \dots, 2$ and $n_4 = 0, 1$). The D^{*0} is reconstructed in the decay mode $D^0\pi^0$ and the D^0 candidate is reconstructed in four decay modes: $D^0 \rightarrow K^-\pi^+, K^-\pi^+\pi^0, K^-\pi^+\pi^-\pi^+, K_S^0\pi^-\pi^+$.

The selection of the fully reconstructed B candidates is made according to the values of two variables:

$$\Delta E = E_B^* - E_{beam} , \quad (3)$$

where E_B^* is the energy of the B meson and E_{beam} is the beam energy, both in the $\Upsilon(4S)$ rest frame; m_{ES} , the energy substituted mass, defined as:

$$m_{ES} = \sqrt{[(s/2 + \mathbf{p} \cdot \mathbf{p}_B)^2/E^2] - |\mathbf{p}_B|^2} , \quad (4)$$

where \sqrt{s} is the total energy of the e^+e^- system in the $\Upsilon(4S)$ rest frame, and (E, \mathbf{p}) and (E_B, \mathbf{p}_B) are the four-momenta of the e^+e^- system and the reconstructed B candidate respectively, both in the laboratory frame. We require $-0.1 < \Delta E < 0.08$ GeV and $m_{ES} > 5.21$ GeV/ c^2 .

For each reconstructed B_{reco} mode i the m_{ES} distribution of the reconstructed B candidates is fit with the sum of an Argus function [5] and a Crystal Ball function [6]. The Argus function models the continuum and combinatorial background whereas the Crystal Ball models the signal component, which peaks at the B mass. The purity of the mode i is defined as $S_i/(S_i + B_i)$, where S_i (B_i) is the number of signal (background) events with $m_{ES} > 5.27$ GeV/ c^2 , as determined by the fit. In events with more than one reconstructed charged B candidate we select the candidate reconstructed in the mode with the highest purity. Figure 1 shows the m_{ES} distribution for all B_{reco} candidates in data. The yield $N_{B^+B^-}$ of the sample containing one B_{reco} is determined as the area of the fitted Crystal Ball function. We obtain $N_{B^+B^-} = (1.67 \pm 0.09) \times 10^5$. The error on $N_{B^+B^-}$ is dominated by systematics and is discussed in Section 4.2.

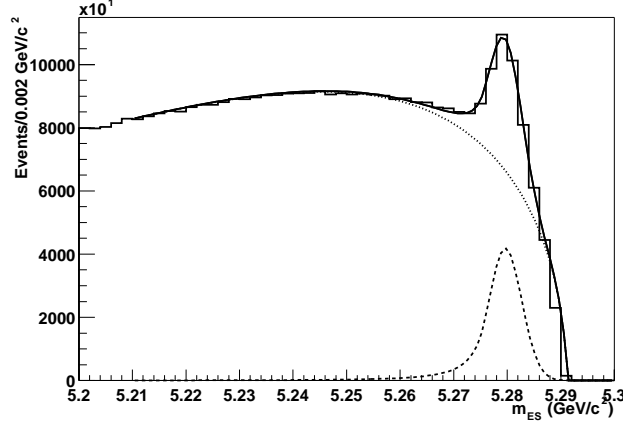


Figure 1: Distribution of the energy substituted mass m_{ES} in data for the fully reconstructed B mesons (histogram). The solid curve shows the result of the fit (see text). Also shown are the signal (dashed curve) and the background (dotted curve) components.

We define the signal region on the B_{reco} side to be $-0.09 < \Delta E < 0.06 \text{ GeV}$ and $m_{\text{ES}} > 5.27 \text{ GeV}/c^2$ and we use the events contained in the sideband $5.21 < m_{\text{ES}} < 5.26 \text{ GeV}/c^2$ as a control sample for continuum and combinatorial background. The same B_{reco} reconstruction technique has been used in other *BABAR* analyses like [7].

3.2 Selection of $B^- \rightarrow \tau^- \bar{\nu}$ decays

In the events where a B_{reco} is reconstructed we search for decays of the recoil B in a τ plus a neutrino; the τ lepton is identified in the following decay channels: $\tau^- \rightarrow e^- \nu \bar{\nu}$, $\tau^- \rightarrow \mu^- \nu \bar{\nu}$, $\tau^- \rightarrow \pi^- \nu$, $\tau^- \rightarrow \pi^- \pi^0 \nu$, $\tau^- \rightarrow \pi^- \pi^+ \pi^- \nu$. All the selection criteria have been optimized to achieve the best upper limit.

The possible modes in which a B_{reco} meson can be reconstructed have been classified by decreasing purity. For each reconstructed τ decay channel we select only B_{reco} mesons reconstructed in the first n modes, where n has been chosen for the best upper limit.

The event total charge q is defined as the sum of the B_{reco} charge plus the τ decay products charge. We consider only events with total charge $q = 0$ (right sign sample). The complementary sample with $|q| = 2$ (wrong sign sample) contains a negligible fraction of the signal and is used as a control sample to test the analysis strategy and the agreement between the selected events in data and the expectation from Monte Carlo simulations.

All the physical quantities mentioned in the following, except where explicitly stated, refer to the recoil B .

3.2.1 Selection of $\tau^- \rightarrow e^- \nu \bar{\nu}$, $\tau^- \rightarrow \mu^- \nu \bar{\nu}$ and $\tau^- \rightarrow \pi^- \nu$ decays

The $\tau^- \rightarrow e^- \nu \bar{\nu}$, $\tau^- \rightarrow \mu^- \nu \bar{\nu}$ and $\tau^- \rightarrow \pi^- \nu$ channels are characterized by a single charged track in the final state coming from the primary vertex.

We require:

- one reconstructed charged track which has not been identified as a kaon, no reconstructed π^0 and no reconstructed K_S^0 ;
- at most one photon candidate with total energy in the laboratory frame less than 110 MeV. Only photons of at least 50 MeV are considered;
- at least 1.2 GeV/c of missing momentum in the laboratory frame;
- the track must be identified as a lepton for the $\tau^- \rightarrow e^- \nu \bar{\nu}$ and $\tau^- \rightarrow \mu^- \nu \bar{\nu}$ selections;
- for the $\tau^- \rightarrow \pi^- \nu$ selection we require the charged track to have a momentum in the recoil B rest frame of at least 1.2 GeV/c and not be identified as either an electron or a muon.

3.2.2 Selection of $\tau^- \rightarrow \pi^- \pi^0 \nu$ decay

The $\tau^- \rightarrow \pi^- \pi^0 \nu$ decay proceeds via an intermediate ρ^- state. We require:

- one reconstructed track which has not been identified as a kaon or a lepton, one reconstructed π^0 and no reconstructed K_S^0 ;
- at least 1.4 GeV/c of missing momentum in the laboratory frame;
- at most one photon candidate with total energy in the laboratory frame less than 100 MeV. Only photons of at least 50 MeV and not used for the π^0 reconstruction are considered;
- the invariant mass of the $\pi^- \pi^0$ pair has to be in the range $0.55 < m_{\pi^- \pi^0} < 1.0$ GeV/ c^2 ;
- for a further rejection of the continuum background, we require the cosine of the angle between the direction of the momentum of the B_{reco} and the thrust vector of the recoil B to be less than 0.9; the thrust orientation is chosen in order to point in the hemisphere opposite to the direction of the recoil B momentum.

3.2.3 Selection of $\tau^- \rightarrow \pi^- \pi^+ \pi^- \nu$ decay

The τ^- decays into three charged tracks via two intermediate resonances. The full decay chain is: $\tau^- \rightarrow a_1^- \nu$, $a_1^- \rightarrow \pi^- \rho^0$, $\rho^0 \rightarrow \pi^+ \pi^-$. We require:

- three reconstructed charged tracks which have not been identified as leptons or kaons, no reconstructed π^0 and no reconstructed K_S^0 ;
- at least 1.2 GeV/c of missing momentum in the laboratory frame;
- at most one photon candidate with total energy in the laboratory frame less than 100 MeV. Only photons of at least 50 MeV and satisfying the quality requirements on the lateral moment [8] to be between 0.05 and 0.50 and on $\Sigma_9/\Sigma_{25} > 0.9$ are considered. The lateral moment is a shape quantity for a neutral cluster and Σ_9/Σ_{25} is the ratio of the energies deposited in the 9 and 25 crystals closest to the cluster centroid. These quality requirements are introduced to improve the description of the neutral energy distribution obtained from Monte Carlo simulations;
- at least one $\pi^- \pi^+$ pair with invariant mass in the range $0.60 < m_{\pi^+ \pi^-} < 0.95$ GeV/ c^2 ;
- invariant mass of the three pions in the range $1.1 < m_{\pi^- \pi^+ \pi^-} < 1.6$ GeV/ c^2 ;
- total momentum of the three pions in the recoil B rest frame greater than 1.6 GeV/c.

3.3 Efficiency and expected background

The selection efficiencies for the τ decay channels we consider in this analysis are determined from detailed Monte Carlo simulations and are summarized in Table 1. We compute the efficiency as the ratio of the number of events surviving each of our selections and the number of events where a B_{reco} has been reconstructed. The efficiency for the $\tau^- \rightarrow \mu^- \nu \bar{\nu}$ channel is three times lower than the efficiency for the $\tau^- \rightarrow e^- \nu \bar{\nu}$ channel because a large fraction of the muon momentum spectrum is below 1 GeV/c, where the muon selection efficiency is low. These muons are not recovered by the pion selection because we require the pion momentum to be at least 1.2 GeV/c in order to reject combinatorial and continuum backgrounds.

In the computation of the total efficiency for each selection we have taken into account the cross-feed from the other τ decay channels reported in Table 1, the requirement that the B_{reco} is reconstructed in the signal region and that the total reconstructed event charge is zero.

Table 1: Efficiency of the different selections (columns) for the most abundant τ decay channels (rows). In case the efficiency is zero we quote a 90% C.L. upper limit. The last two rows show the total efficiency of the single selections, weighted by the decay branching fractions, and the total efficiency. The errors are statistical only. The total efficiency for each selection is: $\epsilon_i = \sum_{j=1}^{n_{dec}} \epsilon_i^j f_j$, where ϵ_i^j is the efficiency of the selection i for the τ decay channel j , $n_{dec} = 7$ is the number of rows in the table and $f_j = \mathcal{B}(\tau \rightarrow j)$ are the τ branching fractions from Ref. [2].

mode	$e\nu\nu$ (%)	$\mu\nu\nu$ (%)	$\pi\nu$ (%)	$\pi^-\pi^+\pi^-\nu$ (%)	$\pi^-\pi^0\nu$ (%)
$e\nu\nu$	22.9 ± 0.6	0 (<0.09)	0.1 ± 0.1	0 (<0.09)	0 (<0.09)
$\mu\nu\nu$	0 (<0.08)	7.4 ± 0.4	2.7 ± 0.2	0 (<0.08)	0.3 ± 0.1
$\pi\nu$	0.6 ± 0.1	0.5 ± 0.1	21.6 ± 0.6	0 (<0.11)	1.0 ± 0.2
$\pi^-\pi^+\pi^-\nu$	0 (<0.15)	0 (<0.15)	0.4 ± 0.1	6.8 ± 0.6	0.1 ± 0.1
$\pi^-\pi^0\nu$	0 (<0.05)	0 (<0.05)	1.2 ± 0.1	0 (<0.05)	6.6 ± 0.3
$\pi^-\pi^0\pi^0\nu$	0 (<0.14)	0 (<0.14)	0 (<0.14)	0 (<0.14)	0.8 ± 0.2
$\pi^-\pi^+\pi^-\pi^0\nu$	0 (<0.03)	0 (<0.03)	0.1 ± 0.1	0 (<0.03)	0.6 ± 0.2
all τ dec.:	4.2 ± 0.1	1.3 ± 0.1	3.2 ± 0.1	0.6 ± 0.1	2.0 ± 0.1
total:	11.3 ± 0.2				

The expected background is determined separately in the right sign and wrong sign samples. It is composed of events from continuum and combinatorial background, and events with a correctly reconstructed B meson. Simulations of $B^0\bar{B}^0$ events have shown that events where a neutral B is incorrectly reconstructed as a charged B provide a negligible peaking component.

The continuum and combinatorial background is determined from the number of events in the m_{ES} sideband, scaled by the ratio of the areas of the fitted Argus function in the signal and sideband regions. Since the number of background events after the full selection is too small to perform a precise fit, we define for each selection criterion a preselection based on the requirements on the number of reconstructed charged tracks and π^0 mentioned in section 3.2. We fit the m_{ES} distribution after each preselection and we assume that the ratio of the fitted Argus in sideband and signal regions, which we use in our estimate of the continuum and combinatorial background, is unchanged after the full selection. The peaking background is determined from Monte Carlo

simulations of B^+B^- events.

Another source of background originates from $e^+e^- \rightarrow \tau^+\tau^-$ events. From Monte Carlo simulations we expect 5.8 ± 1.9 events from $\tau^+\tau^-$ that survive the $\tau^- \rightarrow \pi^- \nu$ selection. No $\tau^+\tau^-$ event survives in the wrong sign sample. The expected background is summarized in Tables 2 and 3 for the wrong sign and right sign samples, respectively. The systematic corrections on the expected background are described in the next Section.

Table 2: Expected background for the wrong sign sample. The peaking component is estimated from inclusive B^+B^- Monte Carlo and the combinatorial plus continuum component from the data sideband. If no event survives the selection we quote a 90% C.L. upper limit on the expected background. Systematic corrections are not included.

selection	peaking	cont. + comb.	total bkg.
$e\nu\nu$	4.6 ± 1.8	0.6 ± 0.4	5.2 ± 1.8
$\mu\nu\nu$	0.7 ± 0.7	$0 (<1.4)$	0.7 ± 0.7
$\pi\nu$	5.3 ± 1.9	$0 (<1.4)$	5.3 ± 1.9
$\pi^-\pi^+\pi^-\nu$	2.0 ± 1.2	2.1 ± 0.8	4.1 ± 1.4
$\pi^-\pi^0\nu$	9.4 ± 2.6	$0 (<1.4)$	9.4 ± 2.6
all			24.7 ± 4.0

Table 3: Expected background for the right sign sample. The peaking component is estimated from inclusive B^+B^- Monte Carlo and the combinatorial plus continuum from the data sideband. The contribution from the $\tau^+\tau^-$ background is also shown. If no event survives the selection we quote a 90% C.L. upper limit on the expected background. Systematic corrections are not included.

selection	peaking	cont. + comb.	$\tau^+\tau^-$ bkg.	total bkg.
$e\nu\nu$	7.2 ± 2.1	$0 (<1.4)$	$0 (<1.5)$	7.2 ± 2.1
$\mu\nu\nu$	4.7 ± 1.8	0.6 ± 0.4	$0 (<1.5)$	5.3 ± 1.8
$\pi\nu$	4.3 ± 1.6	1.3 ± 0.6	5.8 ± 1.9	11.4 ± 2.5
$\pi^-\pi^+\pi^-\nu$	1.6 ± 1.1	3.0 ± 1.0	$0 (<1.5)$	4.6 ± 1.5
$\pi^-\pi^0\nu$	10.3 ± 2.9	1.7 ± 0.7	$0 (<1.5)$	12.0 ± 3.0
all				40.5 ± 5.0

In Fig. 2 we show the neutral energy distribution for events in data and for the expected background. Each distribution refers to a different selection and is obtained applying all the requirements except the one on the neutral energy. The plots show no evidence of signal in data.

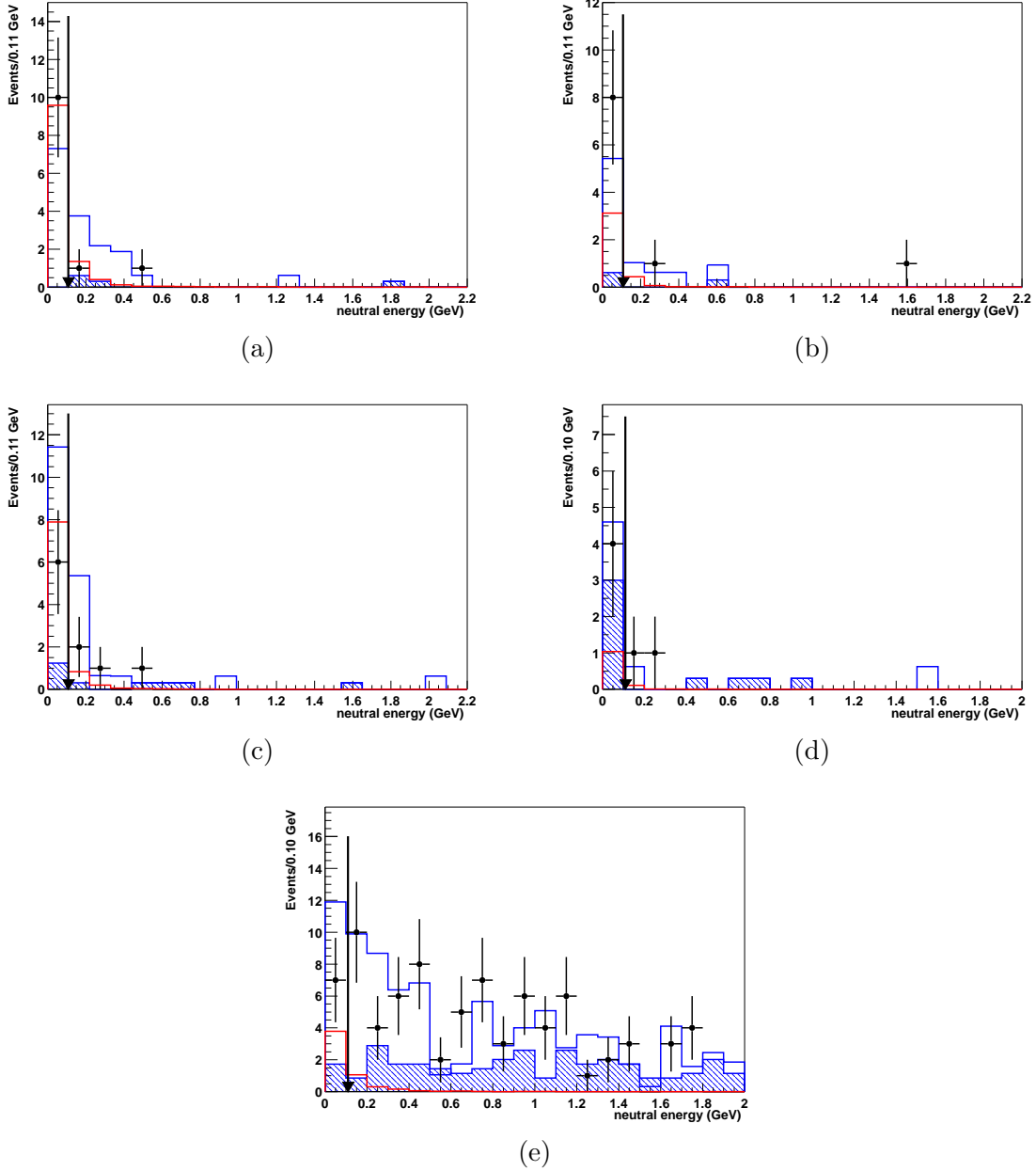


Figure 2: Neutral energy distribution in the laboratory frame after all the selection requirements except the one on the neutral energy for the channels (a) $\tau^- \rightarrow e^- \nu \bar{\nu}$, (b) $\tau^- \rightarrow \mu^- \nu \bar{\nu}$, (c) $\tau^- \rightarrow \pi^- \nu$, (d) $\tau \rightarrow \pi^- \pi^+ \pi^- \nu$ and (e) $\tau \rightarrow \pi^- \pi^0 \nu$. The shaded histogram is the continuum plus combinatorial component of the expected background; the solid histogram represents the peaking component of the expected background and the background from $\tau^+ \tau^-$ events; the dots are the data in the m_{ES} signal region; the red light shaded histogram represents the distribution for Monte Carlo simulated signal events scaled to $\mathcal{B}(B^- \rightarrow \tau^- \bar{\nu}) = 10^{-3}$. The vertical arrow is the requirement on the neutral energy in each selection.

4 Systematic uncertainties

The main sources of uncertainty in the determination of the $B^- \rightarrow \tau^- \bar{\nu}$ branching fraction are:

- uncertainty in the determination of the efficiency ϵ_i for each selection channel;
- uncertainty in the determination of the number of B^+B^- events with one reconstructed B_{reco} $N_{B^+B^-}$;
- uncertainty in the determination of the number of expected background events b_i in each selection channel.

4.1 Uncertainty in the selection efficiencies

The main contributions to the systematic uncertainties in the determination of the efficiencies come from systematic uncertainty on tracking efficiency, neutral reconstruction efficiency and particle identification (PID). Uncertainty in the π^0 reconstruction efficiency introduces an additional 5% contribution to the systematics in the $\tau^- \rightarrow \pi^- \pi^0 \nu$ selection. The different contributions to the systematic uncertainties on the selection efficiencies are reported in Table 4.

Table 4: Contributions to the systematic uncertainty on the efficiency of the different selections. In the $\pi^0 \nu$ channel the contribution to the neutral systematic uncertainty due to π^0 reconstruction is reported explicitly.

selection	tracking (%)	PID (%)	neutral reco (%)	total (%)
$e\nu\nu$	0.8	2.4	0.9	2.7
$\mu\nu\nu$	0.8	6.0	0.9	6.1
$\pi\nu$	0.8	6.0	0.9	6.1
$\pi^- \pi^+ \pi^- \nu$	2.4	11.4	3.8	13.6
$\pi^- \pi^0 \nu$	0.8	3.2	$1.1 \oplus 5$	6.1

4.2 Uncertainty in the determination of $N_{B^+B^-}$

We determine $N_{B^+B^-}$ as the area of the Crystal Ball function fitted to the m_{ES} distribution (see Fig. 1). Using a Gaussian function as an alternative description of the peak, we obtain a value of $N_{B^+B^-}$ which is smaller by 4.5%. We assume this relative difference as the systematic uncertainty on $N_{B^+B^-}$. Using the product of a third order polynomial times an Argus function as an alternative model for the background, the change in $N_{B^+B^-}$ is 0.6%.

4.3 Uncertainty in the expected background and systematic corrections

To take into account possible dependencies of the fitted Argus shape on a given variable used in the selections, we compute a correction factor as the ratio of the expected background events passing the requirement on it using two different approaches. In the first approach we use a single sideband to signal scaling factor (see Section 3.3) determined from a m_{ES} fit over the full variable range. In

the second approach we divide the range of the variable into bins and determine different scaling factors for each bin. To each correction factor we assign 100% of the deviation from unity as a systematic uncertainty.

The expected number of background events after the correction is shown in Tables 5 and 6 for the wrong sign and right sign samples, respectively. It agrees with the number of selected events in data. The total systematic uncertainty amounts to 8.3% for the $\tau^- \rightarrow \mu^- \nu \bar{\nu}$ and $\tau^- \rightarrow e^- \nu \bar{\nu}$ channels, 9.4% for the $\tau^- \rightarrow \pi^- \nu$ channel, 9.9% for the $\tau^- \rightarrow \pi^- \pi^0 \nu$ channel, and 6.1% for the $\tau^- \rightarrow \pi^- \pi^+ \pi^- \nu$ channel.

Table 5: Corrected expected background for the wrong sign sample compared to the number of the selected data candidates. The errors are the statistical and systematic uncertainties.

selection	corr. total bkg.	data candidates
$e\nu\nu$	$4.9 \pm 1.7 \pm 0.4$	5
$\mu\nu\nu$	$0.6 \pm 0.6 \pm 0.1$	3
$\pi\nu$	$5.2 \pm 1.8 \pm 0.5$	0
$\pi^- \pi^+ \pi^- \nu$	$3.8 \pm 1.3 \pm 0.3$	3
$\pi^- \pi^0 \nu$	$8.1 \pm 2.3 \pm 0.9$	9
all	$22.7 \pm 3.7 \pm 1.2$	20

Table 6: Corrected expected background for the right sign sample compared to the number of the selected data candidates. The errors are the statistical and systematic uncertainties.

selection	corr. total bkg.	data candidates	exp. signal events for $\mathcal{B}(B^- \rightarrow \tau^- \bar{\nu}) = 10^{-4}$
$e\nu\nu$	$6.7 \pm 2.0 \pm 0.6$	10	0.7
$\mu\nu\nu$	$5.0 \pm 1.7 \pm 0.4$	8	0.2
$\pi\nu$	$11.2 \pm 2.5 \pm 0.5$	6	0.5
$\pi^- \pi^+ \pi^- \nu$	$4.3 \pm 1.4 \pm 0.3$	4	0.1
$\pi^- \pi^0 \nu$	$10.4 \pm 2.6 \pm 1.0$	7	0.3
all	$37.6 \pm 4.7 \pm 1.3$	35	1.8

5 Upper limit extraction

In order to extract the upper limit on the branching fraction for $B^- \rightarrow \tau^- \bar{\nu}$ we combine the results of the different selections.

We use the likelihood ratio estimator:

$$Q = \frac{\mathcal{L}(s+b)}{\mathcal{L}(b)}, \quad (5)$$

where $\mathcal{L}(s+b)$ and $\mathcal{L}(b)$ are the likelihood functions for signal plus background and background only hypotheses, respectively. The likelihood functions $\mathcal{L}(s+b)$ and $\mathcal{L}(b)$ are defined as:

$$\mathcal{L}(s+b) = \prod_{i=1}^{n_{ch}} \frac{e^{-(s_i+b_i)} (s_i+b_i)^{n_i}}{n_i!}, \quad (6)$$

$$\mathcal{L}(b) = \prod_{i=1}^{n_{ch}} \frac{e^{-b_i} b_i^{n_i}}{n_i!}, \quad (7)$$

where n_{ch} is the number of selection channels, s_i and b_i are the expected number of signal and background events respectively and n_i is the number of selected events in each channel. In particular, s_i can be written in terms of $\mathcal{B}(B^- \rightarrow \tau^- \bar{\nu})$ as:

$$s_i = s \epsilon_i = N_{B^+B^-} \mathcal{B}(B^- \rightarrow \tau^- \bar{\nu}) \epsilon_i, \quad (8)$$

where s is the total expected number of $B^- \rightarrow \tau^- \bar{\nu}$ events, ϵ_i is the selection efficiency for the i -th channel, $N_{B^+B^-}$ is the number of B^+B^- events with one reconstructed B_{reco} .

We have no evidence of signal and we set a 90% C.L. upper limit using a fast parametric Monte Carlo generating random experiments for different values of the branching fraction $\mathcal{B}(B^- \rightarrow \tau^- \bar{\nu})$. The confidence level for the signal hypothesis can be computed as:

$$\text{C.L.}_s = \frac{\text{C.L.}_{s+b}}{\text{C.L.}_b} = \frac{N_{Q_{s+b} \leq Q}}{N_{Q_b \leq Q}}, \quad (9)$$

where $N_{Q_{s+b} \leq Q}$ and $N_{Q_b \leq Q}$ are the number of the generated experiments which have a likelihood ratio less than or equal to the measured one, in the background plus signal and background only hypothesis respectively. The 90% C.L. upper limit to the branching fraction is the value for which $\text{C.L.}_s = 1 - 0.9$. We determine:

$$\mathcal{B}(B^- \rightarrow \tau^- \bar{\nu}) < 6.3 \times 10^{-4}, \quad 90\% \text{ C.L.} \quad (10)$$

In the extraction of the above limit we have included the uncertainty on the efficiency by reducing the efficiencies by one standard deviation (adding in quadrature the statistical and systematic uncertainty), and we have assumed conservatively the estimate of $N_{B^+B^-}$ obtained with a Gaussian model instead of a Crystal Ball.

The statistical and systematic uncertainties on the expected background can be included in the likelihood definition by folding it with a Gaussian distribution having as standard deviation the combined statistical and systematic error on the estimate of b_i . The effect of the uncertainty on the expected background is shown in Fig. 3. Including this uncertainty the upper limit becomes:

$$\mathcal{B}(B^- \rightarrow \tau^- \bar{\nu}) < 7.7 \times 10^{-4}, \quad 90\% \text{ C.L.} \quad (11)$$

The central value of the branching fraction corresponds to the minimum in the likelihood ratio distribution. Using $N_{B^+B^-}$ obtained with a Crystal Ball model and the central values of the efficiencies, we determine $\mathcal{B}(B^- \rightarrow \tau^- \bar{\nu}) = (1.1^{+3.8}_{-1.1} \times 10^{-4})$.

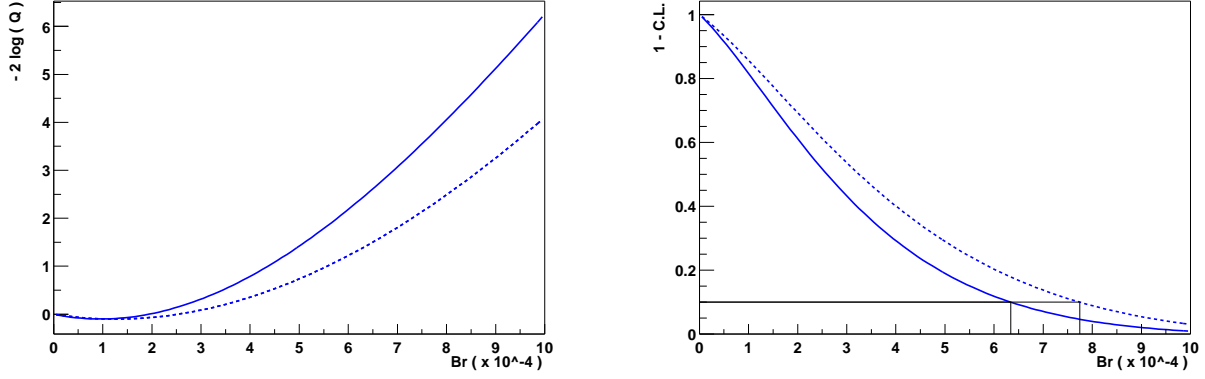


Figure 3: Distributions of the likelihood ratio (left) and confidence level (right) as a function of $\mathcal{B}(B^- \rightarrow \tau^- \bar{\nu})$. The dashed (solid) curve corresponds to the case in which the uncertainty on the expected background is included (not included).

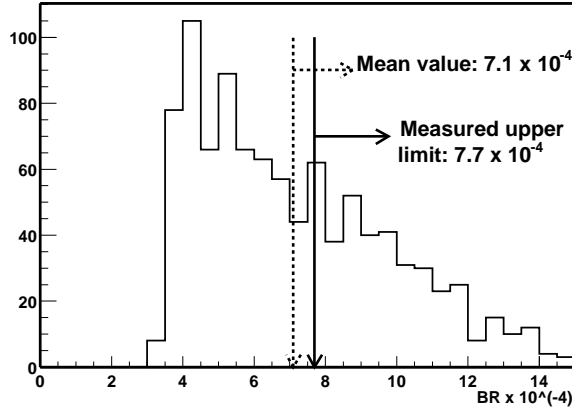


Figure 4: Distribution of the upper limit obtained by generating the selected data events according to Poisson distributions. The statistical and systematic uncertainties on the expected background are taken into account. The dashed line indicates the nominal sensitivity, whereas the solid line shows the upper limit extracted from the data.

If we let the number of selected events in each channel fluctuate according to Poisson distribution with the number of observed events as a mean we obtain the distribution of the possible upper limits shown in Fig. 4. The central value of this distribution (7.1×10^{-4}) represents our sensitivity to the upper limit.

The *BABAR* Collaboration performed also another search for the $B^- \rightarrow \tau^- \bar{\nu}$ decay using a statistically independent sample [9]. The sample is defined by one B^+ meson decaying in $\bar{D}^0 \ell^+ \nu_\ell X$ final state where X is either a photon, π^0 or nothing. The two upper limits have been combined using the statistical technique described above to combine several channels. The combined upper limit is:

$$\mathcal{B}(B^- \rightarrow \tau^- \bar{\nu}) < 4.1 \times 10^{-4}, \text{ 90\% C.L.} \quad (12)$$

6 Summary

A search for $B^- \rightarrow \tau^- \bar{\nu}$ has been performed in the recoil of a fully reconstructed B_{reco} sample. The analysis uses the following τ decay channels: $\tau^- \rightarrow e^- \nu \bar{\nu}$, $\tau^- \rightarrow \mu^- \nu \bar{\nu}$, $\tau^- \rightarrow \pi^- \nu$, $\tau^- \rightarrow \pi^- \pi^0 \nu$ and $\tau^- \rightarrow \pi^- \pi^+ \pi^- \nu$. The results of the search in the different channels have been combined using a likelihood approach. No signal is observed and an upper limit has been set:

$$\mathcal{B}(B^- \rightarrow \tau^- \bar{\nu}) < 7.7 \times 10^{-4}, \text{ 90\% C.L.}$$

The upper limits set by the two independent $B^- \rightarrow \tau^- \bar{\nu}$ searches in the *BABAR* experiment have been combined using the statistical technique described in this paper to obtain the following result:

$$\mathcal{B}(B^- \rightarrow \tau^- \bar{\nu}) < 4.1 \times 10^{-4}, \text{ 90\% C.L.}$$

All results are preliminary.

7 Acknowledgments

We are grateful for the extraordinary contributions of our PEP-II colleagues in achieving the excellent luminosity and machine conditions that have made this work possible. The success of this project also relies critically on the expertise and dedication of the computing organizations that support *BABAR*. The collaborating institutions wish to thank SLAC for its support and the kind hospitality extended to them. This work is supported by the US Department of Energy and National Science Foundation, the Natural Sciences and Engineering Research Council (Canada), Institute of High Energy Physics (China), the Commissariat à l’Energie Atomique and Institut National de Physique Nucléaire et de Physique des Particules (France), the Bundesministerium für Bildung und Forschung and Deutsche Forschungsgemeinschaft (Germany), the Istituto Nazionale di Fisica Nucleare (Italy), the Foundation for Fundamental Research on Matter (The Netherlands), the Research Council of Norway, the Ministry of Science and Technology of the Russian Federation, and the Particle Physics and Astronomy Research Council (United Kingdom). Individuals have received support from the A. P. Sloan Foundation, the Research Corporation, and the Alexander von Humboldt Foundation.

References

- [1] M. Neubert, Phys. Rev. D **45** (1992) 2451; A. Kronfeld, talk given at “9th International Symposium on Heavy Flavor Physics” hep-ph/0111376.
- [2] Particle Data Group, K. Hagiwara *et al.*, Phys. Rev. D **66**, 010001 (2002).
- [3] M. Acciarri *et al.*, L3 Collaboration, Phys. Lett. **B396** (1997) 327-337.
- [4] The *BABAR* Collaboration, A. Palano *et al.*, Nucl. Instrum. Methods **A479**, 1 (2002).
- [5] ARGUS Collaboration, H. Albrecht *et al.*, Phys. Lett. **B185**, 218 (1987).

[6] The Crystal Ball function is defined as:

$$f(x) = N \cdot \begin{cases} \exp(-\frac{(x-\bar{x})^2}{2\sigma^2}) & ; (\bar{x} - x)/\sigma > \alpha \\ A \times (B - \frac{x-\bar{x}}{\sigma})^{-n} & ; (\bar{x} - x)/\sigma \leq \alpha \end{cases}$$

where $A \equiv \left(\frac{n}{|\alpha|}\right)^n \times \exp(-|\alpha|^2/2)$ and $B \equiv \frac{n}{|\alpha|} - |\alpha|$. N is a normalization factor, \bar{x} and σ are the peak position and width of the Gaussian portion of the function, α is the point at which the function changes to the power function and n is the exponent of the power function. A and B are defined so that the function and its first derivative are continuous at α .

[7] The *BABAR* Collaboration, B.Aubert *et al.*, “A search for $B^- \rightarrow K^- \nu \bar{\nu}$ ”, *BABAR-CONF-03/006*, SLAC-PUB-9710.

[8] A. Drescher, *et al.*, Nucl. Instr. Meth. A **237**, 464(1985).

[9] The *BABAR* Collaboration, B.Aubert *et al.*, “A Search for $B^+ \rightarrow \tau^+ \nu_\tau$ Recoiling Against $B^- \rightarrow D^0 \ell^- \bar{\nu}_\ell X$ ”, *BABAR-CONF-03/005*, SLAC-PUB-9688.